Modeling of Raw Material Mixing Process in Raw Meal Grinding Installations

TSAMATSOULIS DIMITRIS
Halyps Building Materials S.A., Italcementi Group
17th Klm Nat. Rd. Athens – Korinth
GREECE
d.tsamatsoulis@halyps.gr http://www.halyps.gr

Abstract: - The objective of the present study is to build a reliable model of the dynamics among the chemical modules in the outlet of raw meal grinding systems and the proportion of the raw materials. The process model is constituted from three transfer functions, each one containing five independent parameters. The computations are performed using a full year industrial data by constructing a specific algorithm. The results indicate high parameters uncertainty due to the large number of disturbances during the raw mill operation. The model developed can feed with inputs advanced automatic control implementations, in order a robust controller to be achieved, able to attenuate the disturbances affecting the raw meal quality.

Key-Words: - Dynamics**,** Raw meal, Quality, Mill, Grinding, Model, Uncertainty

1 Introduction

The main factor primarily affecting the cement quality is the variability of the clinker activity [1] which depends on the conditions of the clinker formation, raw meal composition and fineness. A stable raw meal grinding process provides a low variance of the fineness.

recycle elevator feeds the separator. The material in the mill and classifier are dried and dedusted by hot gas flow.

An unstable raw mix composition not only has impact on the clinker composition but also affects the kiln operation and subsequently the conditions of the clinker formation. So it is of high importance to keep the raw meal quality in the kiln feed as much

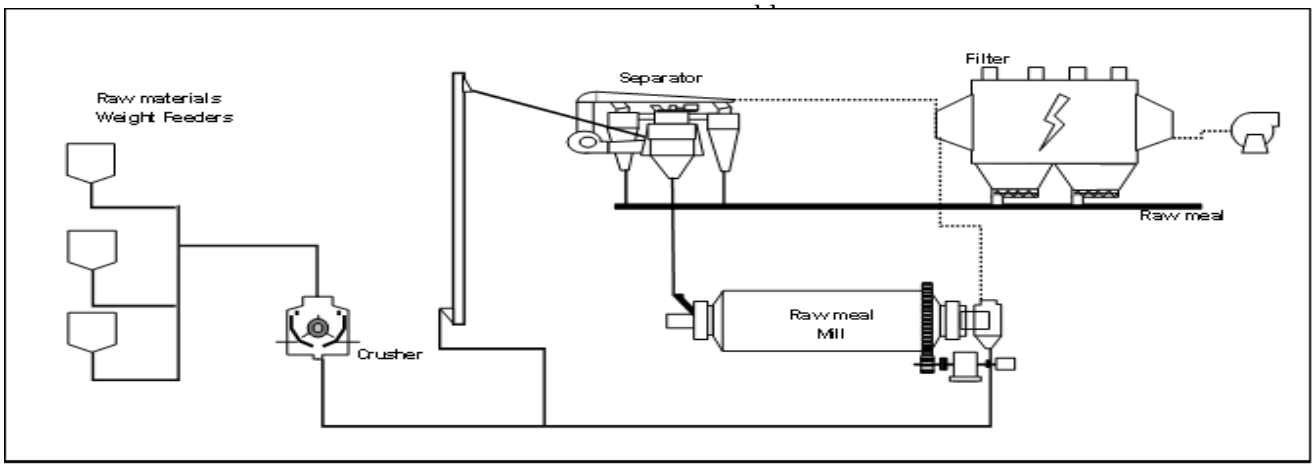

Figure 1. Flow chart of raw meal production

Figure 1 depicts a typical flow chart of raw meal production. In the demonstrated closed circuit process, the raw materials' feeding is performed via three weight feeders, feeding first a crusher. The crusher outlet goes to the recycle elevator and from there to a dynamic separator, the speed and gas flow of which controls the product fineness. The fine exit stream of the separator is the main part of the final product. The coarse separator return, is directed to the mill, where is ground and from there via the

The variation of this parameter is related to the homogeneity of the raw materials in the raw mill (RM) inlet, the mixing efficiency of the homogenizing silo and the regulation effectiveness as well. Due to its complexity and significance, different automated systems are available for sampling and analyzing the raw mix as well as for adjustment of the mill weight feeders according to the raw meal chemical modules in the RM outlet. The regulation is mainly obtained via PID and

adaptive controllers. Ozsoy et al. [2] developed three different linear multivariable stochastic ARX (AutoRegressive with eXogenous input) models to describe the dynamics of a raw blending system. Kural et al. [3] built on stochastic multivariable dynamic models and designed model predictive controllers to calculate the optimal feed ratios of the raw materials despite disturbances. As clearly the authors declare the disturbances coming from the variations in the chemical compositions of the raw materials from long-term average compositions cause the changes of the system parameters. Several adaptive controllers of varying degrees of complexity have been also developed [4, 5]. Banyasz at al. [5] presented the control algorithm in a technology-independent manner. Duan et al. [6] presented a case study on the practical implementation of a hybrid expert system for a raw materials blending process. Tsamatsoulis [7] tuned a classical PID controller among chemical modules in the RM output and raw materials proportion in the mill feed, using as optimization criterion the minimum standard deviation of these modules in the kiln feed. He concluded that the application of stability criteria is necessary. He also proved that the variance of the kiln feed composition not only depends on the raw materials variations and the mixing capacity of the silos but also is strongly related with the effectiveness of the regulating action. The reason that so intensive efforts are devoted to the raw meal regulation is that advanced raw mill control delivers improved economic performance in cement production, as Gordon [8] points out.

The common field among all these attempts and designs is the assumption of a model describing the process dynamics. As Jing et al. state [9], modeling of the uncertainties or handling the deterministic complexity are typical problems frequently encountered in the field of systems and control engineering. For this and other reasons in [10] special attention is paid to the problems of synthesis of dynamical models of complex systems, construction of efficient control models, and to the development of simulation. As a result, to design a robust controller, satisfying a given sensitivity constraint [11, 12, 13] an efficient modeling of the process is obligatory.

The aim of the present study is to develop a reliable model of the dynamics between the raw meal modules in the RM outlet and the proportions of the raw materials in the feeders for an existing closed circuit RM of the Halyps plant. Due to the uncertainty of the materials composition, it is necessary not only to describe the mixing process using a representative model, but to estimate the parameters uncertainty as well. The model coefficients and their uncertainty are computed exclusively from routine process data without the need of any experimentation as usually the model identification needs. Then, this process model can be utilized to build or to tune a large variety of controllers able to regulate this challenging industrial process.

2 Process Model

2.1 Proportioning Moduli Definition

The proportioning moduli are used to indicate the quality of the raw materials and raw meal and the clinker activity too. For the main oxides, the following abbreviations are commonly used in the cement industry: C=CaO, S=SiO_2, A=Al_2O_3, F=Fe_2O_3. The main moduli characterizing the raw meal and the corresponding clinker are as follow [1]:

$$Lime\ Saturation\ Factor$$
$$LSF = \frac{100 \cdot C}{2.8 \cdot S + 1.18 \cdot A + 0.65 \cdot F} \quad (1)$$

$$Silica\ Modulus\ \ SM = \frac{S}{A + F} \quad (2)$$

$$Alumina\ Modulus\ \ AM = \frac{A}{F} \quad (3)$$

The regulation of some or all of the indicators (1) to (3) contributes drastically to the achievement of a stable clinker quality.

2.2 Block Diagram

Limestone and clay are fed to the mill via two silos: the first silo contains limestone while the second one mixture of limestone and clay with volume ratio clay: limestone=2:1. This composite material is considered as the "clay" material of the process. The third silo contains either the corrective material of high iron oxide or high alumina content or both of them. The block diagram is illustrated in Figure 2, where the controller block also appears.

Each block represents one or more transfer function: G_c symbolizes the transfer function of the controller. With G_{mill}, the RM transfer function is indicated, composed from three separate functions. During the sampling period, a sampling device accumulates an average sample. The integrating action of the sampler during the time interval between two consecutive samples is denoted by the

function G_s. The delay caused by the sample analysis is shown by the function G_M. The silo transfer function is depicted by G_{silo}.

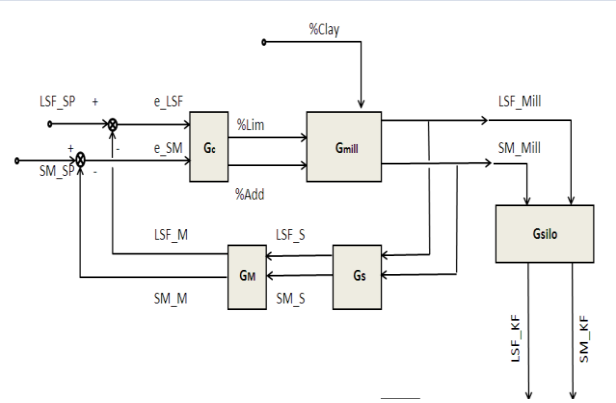

Figure 2. Flow chart of the grinding and blending process.

%Lim, %Add, %Clay = the percentages of the limestone, additive and clay in the three weight feeders. LSF_{Mill}, SM_{Mill} = the spot values of LSF and SM in the RM outlet, while LSF_S, SM_S, LSF_M, SM_M = the modules of the average sample and the measured one. Finally LSF_{KF}, SM_{KF} = the corresponding modules in the kiln feed. The LSF and SM set points are indicated by LSF_{SP} and SM_{SP} respectively, while e_LSF and e_SM stand for the error between set point and respective measured module.

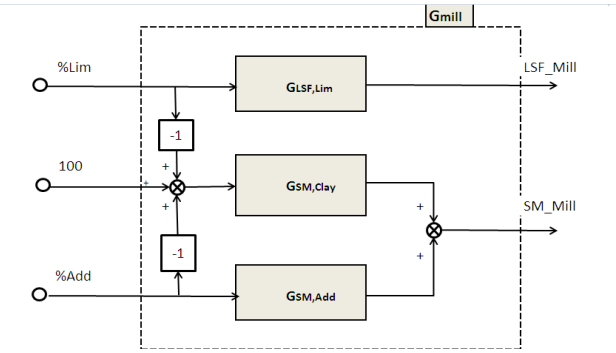

Figure 3. Transfer functions of the RM block.

The transfer function of the raw meal mixing in the RM is analyzed in more detail in Figure 3.The functions between the modules and the respecting percentages of the raw materials are indicated by $G_{LSF,Lim}$, $G_{SM,Clay}$, $G_{SM,Add}$. This configuration includes some simplifications and assumptions which are proved as valid in connection with the current raw materials analysis:

- There is not impact of the limestone to SM as the S, A, F content of limestone is in general very low compared with the other raw materials.
- Moreover there is not effect of the additive on the LSF as its percentage is very low, less than 3%.
- The materials humidity is neglected, to simplify the calculations.
- As to the clay, the function %Clay=100-%Lim-%Add is taken into account.

2.3 Process Transfer Functions

For the existing RM circuit, the objective of the analysis is to model the transfer function between the raw meal modules in the RM outlet and the proportions of the raw materials in the feeders. Consequently only for the functions G_{mill}, G_s, G_M analytical equations in the Laplace domain are needed. The G_M represents a pure delay, therefore is given by equation (4):

$$G_M = e^{-tM \cdot s} \tag{4}$$

The delay t_M is composed by the time intervals of sample transferring, preparation, analysis and computation of the new settings of the three feeders and finally transfers of those ones to the weight scales. For the given circuit the average t_M = 25 min = 0.42 h. By the application of the mean value theorem and the respective Laplace transform, the function G_s is calculated by the formula (5):

$$G_s = \frac{1}{T_s \cdot s}(1 - e^{-Ts \cdot s}) \tag{5}$$

The sampling period T_s is equal to 1 h. Based on the step response results of [7], performed in the same RM a second order with time delay (SOTD) model is chosen for each of the functions $G_{LSF,Lim}$, $G_{SM,Clay}$, $G_{SM,Add}$ described by the equation (6):

$$G_x = \frac{k_{g,x}}{\left(1 + T_{0,x} \cdot s\right)^2} \cdot e^{-td,x \cdot s} \tag{6}$$

Where x = Lim, Clay or Add. The constant k_g, T_0, t_d symbolize the gain, the time constant and the time delay respectively. The value of these nine variables shall be estimated. As measured inputs and outputs of the process are considered the %Lim and %Add as well as LSF_M and SM_M. In the time domain the functions (4)-(6) are expressed by the following equations:

$$LSF_M(t) = LSF_S\,(t - t_M)$$
$$SM_M(t) = SM_S\,(t - t_M) \tag{7}$$

$$LSF_S(t) = \frac{1}{T_s}\int_{t-Ts}^{t} LSF_{Mill}\,dt$$

$$SM_s = \frac{1}{T_s}\int_{t-Ts}^{t} SM_{Mill}\,dt \quad (8)$$

The function between LSF and limestone in the time domain is given by equation (9):

$$LSF - LSF_0 = k_{g,Lim}\cdot\left(1-\exp\left(-\frac{t-t_{d,Lim}}{T_{0,Lim}}\right)-\frac{t-t_{d,Lim}}{T_{0,Lim}}\cdot\exp\left(-\frac{t-t_{d,Lim}}{T_{0,Lim}}\right)\right)\cdot(Lim-Lim_0) \quad (9)$$

The Lim_0 and LSF_0 parameters stand for the steady state values of the input and output variables. The corresponding function between SM, %Clay and %Add is described by equation (10)

$$SM - SM_0 = k_{g,Clay}\cdot\left(\begin{array}{c}1-\exp\left(-\frac{t-t_{d,Clay}}{T_{0,Clay}}\right)\\ -\frac{t-t_{d,Clay}}{T_{0,Clay}}\cdot\exp\left(-\frac{t-t_{d,Clay}}{T_{0,Clay}}\right)\end{array}\right)\cdot(Clay-Clay_0)+k_{g,Add}\cdot\left(\begin{array}{c}1-\exp\left(-\frac{t-t_{d,Add}}{T_{0,Add}}\right)-\frac{t-t_{d,Add}}{T_{0,Add}}\\ \cdot\exp\left(-\frac{t-t_{d,Add}}{T_{0,Add}}\right)\end{array}\right)\cdot(Add_0-Add) \quad (10)$$

The $Clay_0$, Add_0 and SM_0 parameters correspond to the steady state values. $Clay_0$ is not an independent variable but given from the difference 100- Lim_0-Add_0. To avoid elevated degrees of freedom the following equalities are considered:

$$T_{0,Clay} = T_{0,Add} \quad t_{d,Clay} = t_{d,Add} \quad (11)$$

The output y is derived from the input signal u, by applying the convolution between the input and the system pulse function, g, expressed by (12).

$$y(t) - y_0 = \int_0^t (u(\tau)-u_0)\cdot g(t-\tau)d\tau \quad (12)$$

The SM in the mill output is computed from the sum of the two convolution integrals.

2.4 Parameters Estimation Procedure

Each of the three transfer function G_x, defined by the formulae (6) in frequency domain or (9) and (10) in time domain contains five unknown parameters: The gain k_g, the time constant T_0, the delay time t_d and the steady state process input and output u_0 and y_0 respectively. The determination of these coefficients is obtained via the following procedure:

(i) One full year hourly data of feeders' percentages and proportioning moduli are accessed from the plant data base. As basic data set the hourly results of 2009 are taken. The size of the population is 4892 analysis.

(ii) For each pair of input and output and using convenient software, continuous series of data are found. Because for each one of the three functions, five parameters need determination, the minimum acceptable number of continuous in time data is set to ≥14.

(iii) For each mentioned pair, the average number of data of the uninterrupted sets is 18 and the total number of sets is more than 200. Therefore the sample population is high enough, to derive precise computation of both the average parameter values and their uncertainty.

(iv) For each data set and using non linear regression techniques, the five parameters providing the minimum standard error between the actual and calculated values are estimated. For the optimum group of parameters the regression coefficient, R, is also computed.

(v) A minimum acceptable R_{min} is defined. The results are screened and only the sets having $R \geq R_{min}$ are characterized as adequate for further processing. The usual causes of a low regression coefficient are random disturbances inserted in the process or changes in the dynamics during the time interval under examination.

(vi) For the population of the results presenting $R \geq R_{min}$, the average value and the standard deviation of each model parameter are determined. The standard deviation is a good measure of the parameters uncertainty.

3 Results and Discussion

3.1 Model Adequacy

There are various sources of disturbances and uncertainties affecting the ability to model the

process dynamics. As main causes of such variances can be characterized the following:

(i) The limestone and clay unstable composition. The average LSF of 140 limestone samples taken during a full year is 840 with a standard deviation of 670. The respective average LSF of 480 samples of clay is 17 with a standard deviation of 5.This large uncertainty not only has an impact on the gain value, but also on the process time constant and delay.

(ii) The variance of the raw materials moisture. For the same samples referred in (i), the limestone humidity is 3.4±1.2, while the clay one is 10.2±1.7.

(iii) Disturbances of the RM dynamics caused by various conditions of grinding. For example variations of the gas flow and temperature, of the RM productivity, of the circulating load, of the raw mix composition etc.

(iv) Some uncertainty of the time needed for sample preparation and analysis.

(v) Some noise introduced in the measurement during the sample preparation and analysis procedure. Because of this noise and according to the laboratory data, the long term reproducibility of LSF is 0.95.

Due to all these unpredicted disturbances and the resulting uncertainties, to investigate the model adequacy, the cumulative distributions of the regression coefficients are determined for each one of the dynamics. The function between raw materials and SM is a two inputs single output process (TISO). The two cumulative distributions are depicted in Figure 4 computed from a total of 202 data sets.

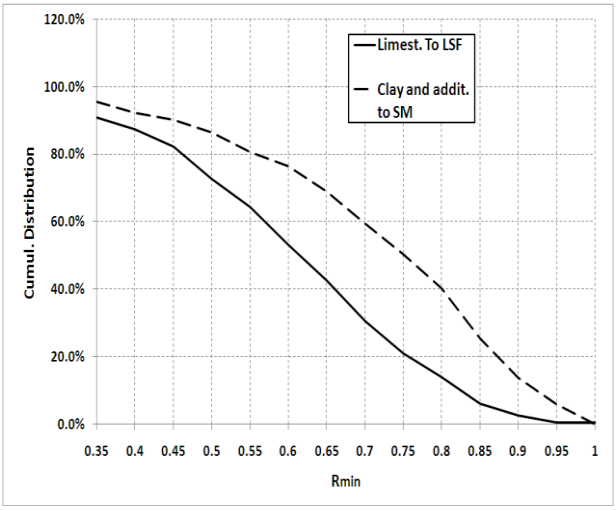

Figure 4. Cumulative distributions of the regression coefficients.

If as minimum acceptable level for good regression a value of R_{min} equal to 0.7 is chosen, then only 30% of the experimental sets present $R \geq R_{min}$ for the dynamics from %limestone to LSF. For the second dynamic the percentage is noticeably higher - ~58%. The TISO treatment among clay, additive and SM results in a very reliable model. It must be noted that the change of the clay percentage results in a disturbance of the dynamics from %additive to SM. The same impact has a change of the additive percentage on the dynamics from %clay to SM. In the case that the model parameters were calculated separately from each material to SM – SISO model - then the percentage of $R \geq 0.7$ is significantly lower than 58%. As to %Clay to SM dynamics the percentage is only 24.5% while the respective percentage from %Additive to SM reaches the 30%, both significantly lower than the result of the TISO model.

Subsequently the effect of the different disturbances on the model identification becomes clear. On the other hand the model describes adequately the blending process during the grinding of the raw mix in the closed RM circuit, for at least the one third of the data sets. For further calculations $R_{min}=0.7$ is selected. One probable cause of this result is the sample size: Bigger the size, higher the probability a disturbance to be inserted to the system. To investigate deeper the above behaviour, for each set of M continuous data a subset of N=14 consecutive samples is taken using a moving window technique. For example if a set contains M=20 samples then M-N+1 new subsets are derived and the dynamic parameters are determined. In this way the total number of sets is increasing to 1155. The computations for LSF dynamics are performed over all the above sets and the distribution of the regression coefficients is shown in Figure 5. In the same figure the distribution of R for the continuous data sets of minimum size 14 also appears. As it can be seen there is a substantial improvement of the model reliability if the size of the population is restricted to 14: The sets possessing $R \geq 0.7$ are the 45.7% of the total population. The respective results for the SM dynamics are depicted in Figure 6.

To verify this positive trend of enhancement of the model consistency to describe the process, previous years data are also extracted and the same distributions shown in Figure 5 are derived. The results are depicted in Table 1. The distribution of the regression coefficients for 2008 data is demonstrated in Figure 7.

From these results it becomes clear that the reduction of the sample size to 14 contributes strongly to the improvement of the model reliability.

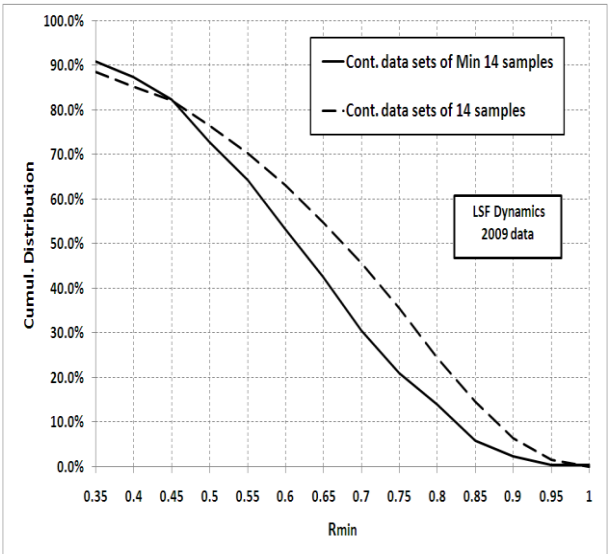

Figure 5. Distribution of the regression coefficients for LSF dynamics and 2009 data.

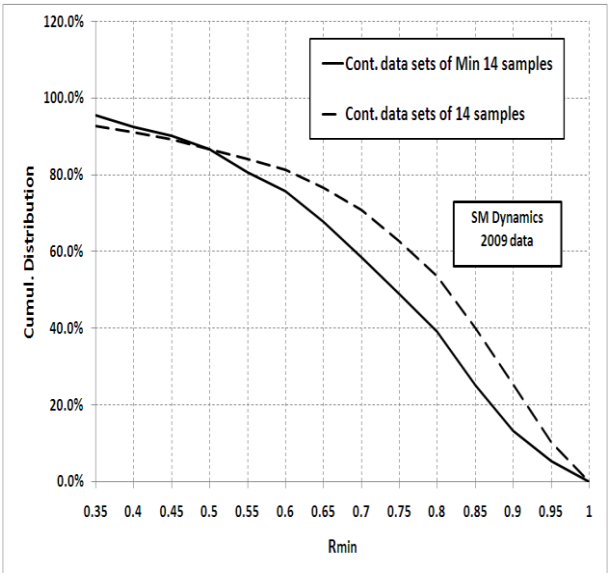

Figure 6. Distribution of the regression coefficients for SM dynamics and 2009 data.

Table 1. Function of the Model Regression Coefficient with the set size

		Sets with Size ≥14		Sets with Size = 14	
	Work. hours	Num. of sets	%Sets with R ≥ 0.7	Num. of sets	%Sets with R ≥ 0.7
2006	6617	185	57.8	3498	68.7
2007	6109	225	43.1	2516	62.6
2008	5928	234	53.8	2024	70.3
2009	4892	202	30.0	1155	45.7

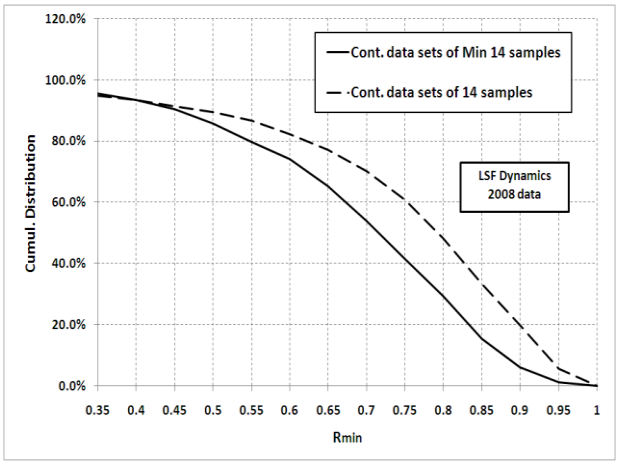

Figure 7. Distribution of the regression coefficients for LSF dynamics and 2008 data.

3.2 Correlations between the model parameters and regression coefficient

As concluded from previous section, the model adequacy depends strongly on the sample size, due to the higher probability a disturbance to be inserted to the system, as bigger the sample size is. For this reason it shall be initially investigated if there is any correlation between the model parameters and the regression coefficient, R. To obtain the above the following procedure is followed.

(i) For all the sets of the parameters and the respective regression coefficients, the range of R, [0,1] is partitioned in intervals of length 0.05.

(ii) Within each interval, the average parameter value is determined

(iii) The results are plotted to facilitate the search of any existing correlation.

The parameters of the LSF transfer function against R are shown in Figures 8 to 10. Both parameter sets for sample size M ≥ 14 and M = 14 are depicted.

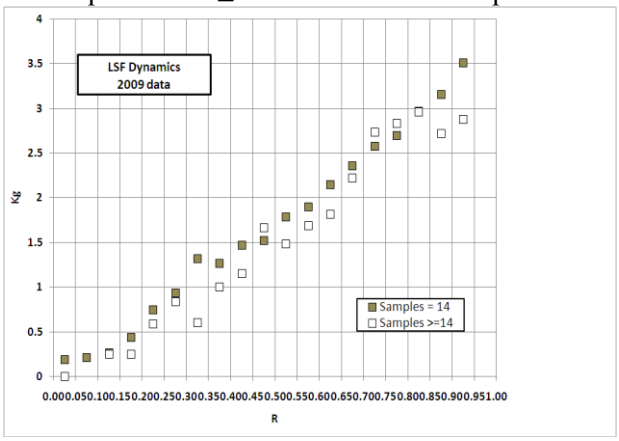

Figure 8. Function between gain of LSF dynamics and R – 2009 data.

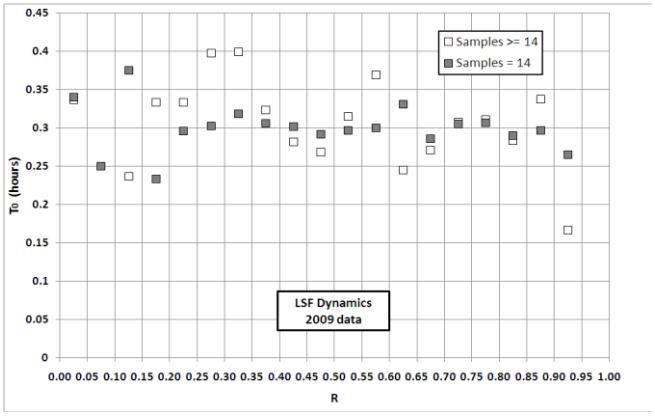

Figure 9. Function between time constant of LSF dynamics and R – 2009 data.

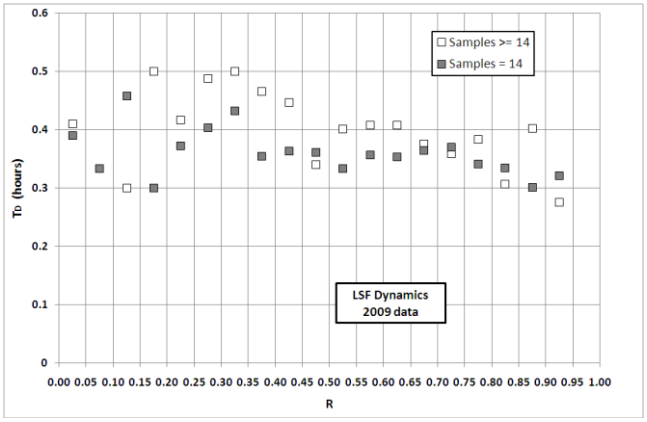

Figure 10. Function between delay time of LSF dynamics and R – 2009 data.

The respective results from %clay and %additive to SM are indicated in Figures 11 to 14.

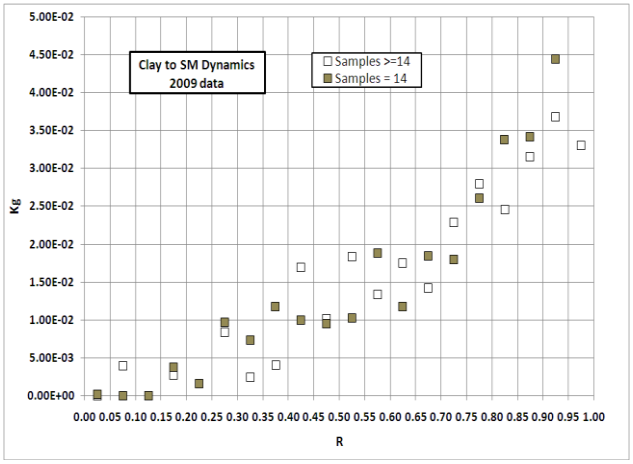

Figure 11. Function between gain of %Clay to SM dynamics and R – 2009 data.

From these figures some essential conclusions can be extracted: While there is not any correlation between the model regression coefficients and the time constant or delay times, the R is strongly and monotonically related with the gains of both models.

As the regression coefficient becomes better, the respective gain increases. Higher regression coefficient implies fewer and weaker disturbances inserted to the system and vice versa. Therefore as more intensive the disturbances are, lower and consequently erroneous the gain is. The above is an additional reason to select a threshold for the R_{min}, to achieve a more accurate set of dynamic parameters.

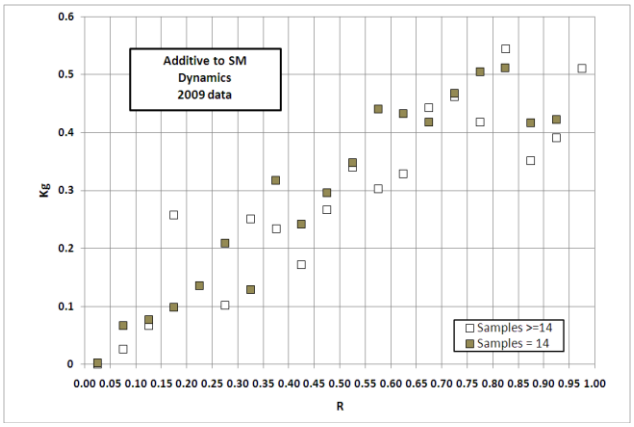

Figure 12. Function between gain of %additive to SM dynamics and R – 2009 data.

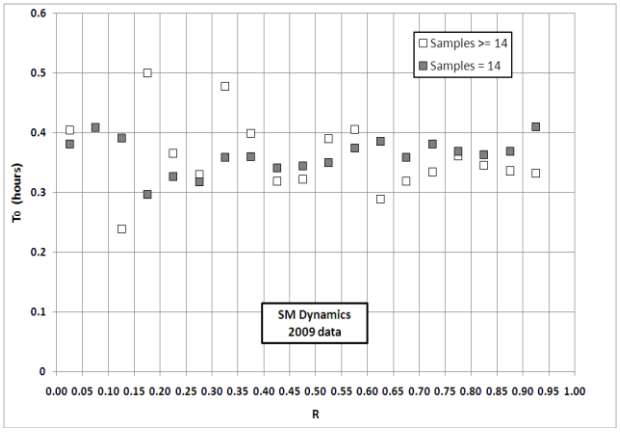

Figure 13. Function between time constant of SM dynamics and R – 2009 data.

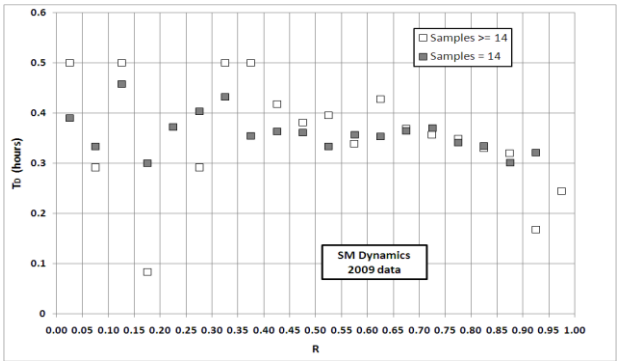

Figure 14. Function between delay time of SM dynamics and R – 2009 data.

To verify this strong trend between model gain and regression coefficient all the k_g and R data of

the years 2006-2009 for sample size M=14 are plotted in Figure 15 for the LSF dynamics. The two variables show high degree of correlation is spite that the slope is not the same for the four years, due to changes of the raw materials composition. So it is absolutely reasonable for further processing to use the dynamic parameters of the sets presenting $R \geq 0.7$

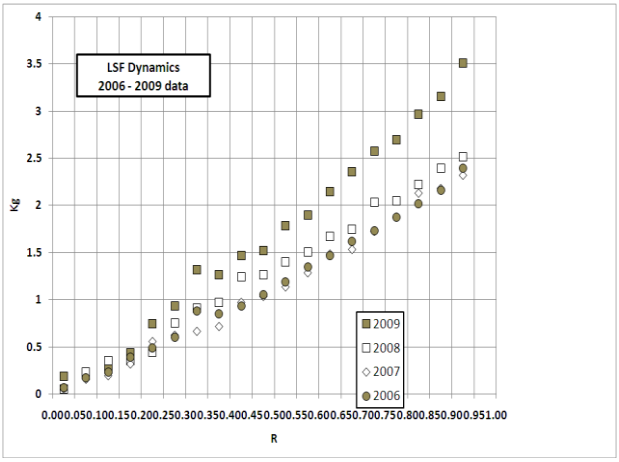

Figure 15. Function between gain of LSF dynamics and R – 2009 data

3.3 Function between the steady state parameters

To evaluate if there is any function between the steady state parameters the next steps are followed.

(i) All the parameters of 2009 data, for sample size M=14 are considered for $R \geq 0.7$.

(ii) The functions LSF_0 = f (Lim_0) and SM_0 = f (Add_0) are investigated.

(iii) The range of Lim_0 is partitioned in intervals of length equal to 2.

(iv) The mean and standard deviation of LSF_0, m and s respectively, are computed for each Lim_0 interval.

(v) The same processing is performed for Add_0, partitioning the range to 0.025 length intervals.

(vi) The low and high limits of the average module are computed, using the formulae $(LL, HL)^T = (m-s, m+s)^T$.

(vii) The results are depicted in Figures 16, 17.

From the Figure 16, a clear correlation between Lim_0 and LSF_0 is concluded. As Lim_0 increases, LSF_0 also augments. The variance of each individual point is due to the raw materials variance and model mismatch because of non - linearities inserted to the process. This plot can be considered as the static gain function between the %Limestone and LSF steady state values. On the contrary Add_0 and SM_0 seem to be independent. The reason of this result is the impact of the Clay_0 on the SM_0.

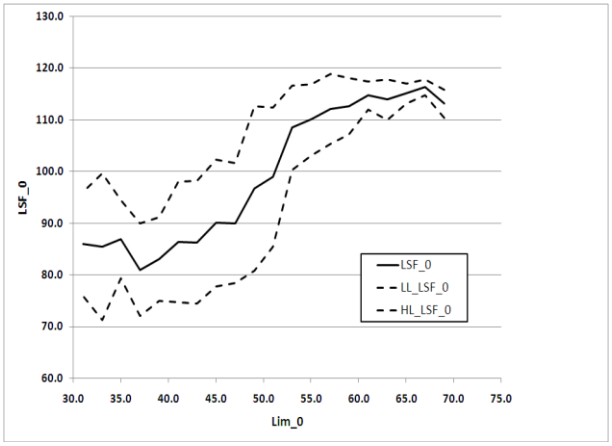

Figure 16. Function between Lim_0 and LSF_0.

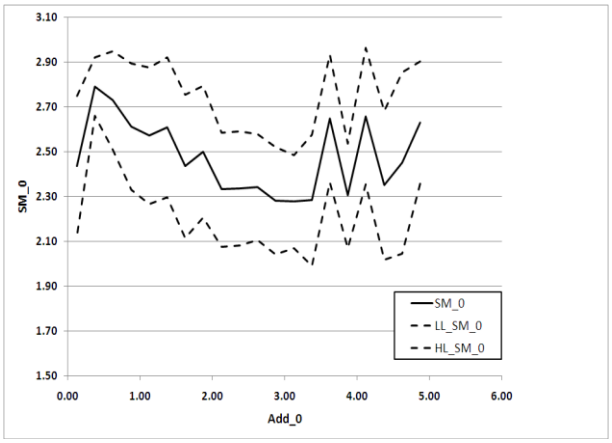

Figure 17. Function between Add_0 and SM_0.

3.4 Variance analysis of the model parameters.

The fundamental motivation to develop a model between the RM feeders and the chemical modules in the mill outlet is the prospect to tune off line an optimum controller - usually PID type - or to utilize the model on line for model predictive control (MPC) purposes. In both cases the variance of the model parameters is of high importance. The knowledge of their uncertainty can lead to a robust controller tuned off line. In the case that MPC is to be implemented, previous information about the magnitude of the parameters change as function of time, can lead to a more effective design.

Therefore a variance analysis of the model parameters it is expected to offer valuable information. To evaluate their natural variability as well as their time evolution, the standard ISO 8258:1991[14] is applied. By implementing this approach mean $\bar{X}$ charts and range R-charts are constructed. The parameters natural standard deviation, σ_{Nat}, is also estimated. The above statistics are computed by following the next steps:

(a) Calculate the absolute range R_i between two consecutive parameters X_i, X_{i-1} and the average range R_{Aver}, over all the ranges population, by applying the equations (13):

$$R_i = |X_i - X_{i-1}| \qquad R_{Aver} = \frac{\sum_{i=1}^{N} R_i}{N} \tag{13}$$

(b) Calculate the maximum range, R_{Max}, for 99% probability provided by the formula (14). Each $R > R_{Max}$ is considered as an outlier and the values are excluded from further calculations.

$$R_{Max} = 3.267 \cdot R_{Aver} \tag{14}$$

(c) After the exclusion of all the outliers and calculation of a final R_{Aver}, the process natural deviation concerning the parameter under investigation is calculated using the equation (15):

$$\sigma_{Nat} = 0.8865 \cdot R_{Aver} \tag{15}$$

(d) The upper and lower control limit – HL and LL respectively - of the mean $\bar{X}$ are computed from the equations (16):

$$LL = \bar{\bar{X}} - 1.88 \cdot R_{Aver}$$
$$HL = \bar{\bar{X}} + 1.88 \cdot R_{Aver} \tag{16}$$

For parameters calculated for sample size M ≥ 14 and M = 14 $\bar{X}$ and R-charts are determined. The gain charts for %limestone to LSF dynamics are demonstrated in Figures 18, 19 for 2009 data. The respective gain charts from %additive to SM transfer function are shown in Figures 20 and 21.

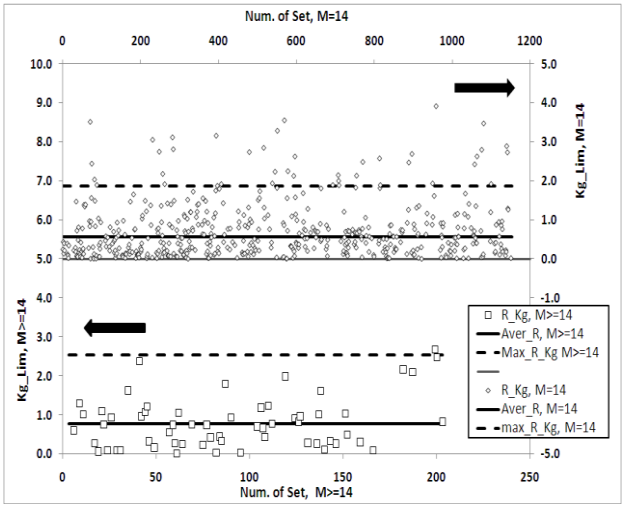

Figure 18. Gain R-chart of LSF dynamics.

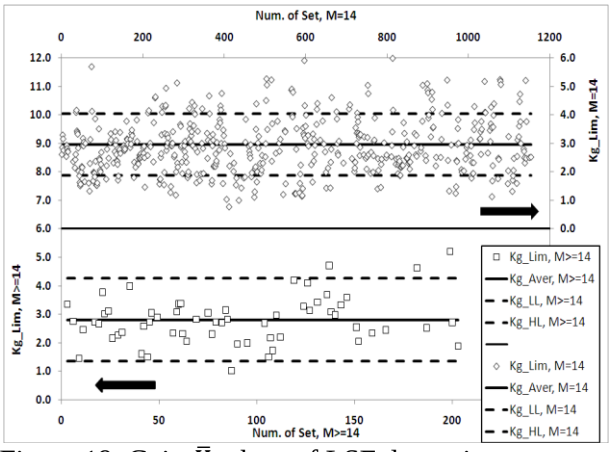

Figure 19. Gain $\bar{X}$ -chart of LSF dynamics.

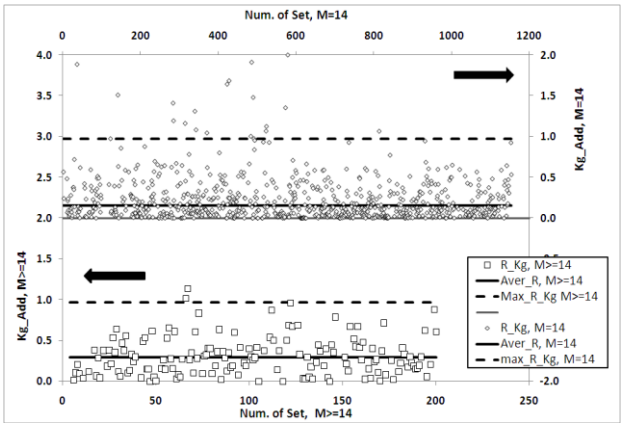

Figure 20. Gain R-chart of %Additive to SM transfer function.

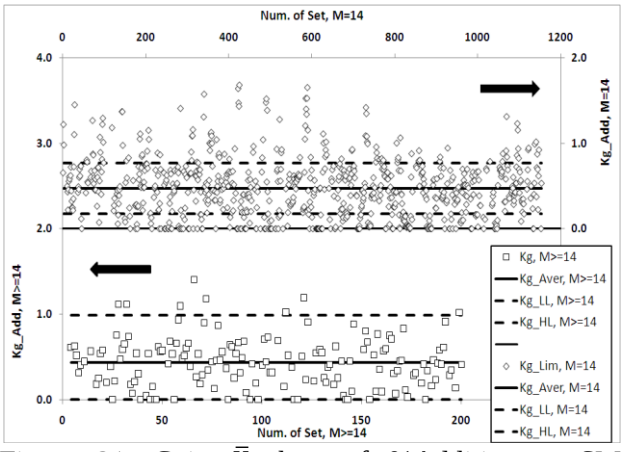

Figure 21. Gain $\bar{X}$ -chart of %Additive to SM transfer function.

Based on these figures and as concerns the average gain range between two consecutive sets, the passing from a sample size M ≥ 14 to M=14 results is a severe decrease of the R_{Aver} and subsequently tighter LL and HL values of the parameter average: The process of gain determination is better controlled, if an adequate but not large population of results is chosen. To investigate in a more thorough manner this result,

the average and natural deviation of each model parameter is calculated over all the results available as to LSF dynamics and 2009 data as regards the SM dynamics. The results are shown in Table 2.

Table 2. Average and σ_{nat} of the model parameters

	Aver.	$\sigma_{nat,1}$	Aver.	$\sigma_{nat,2}$	$\sigma_{nat,2}/\sigma_{nat,1}$
	M ≥ 14		M=14		
	2009				
$K_{g,Lim}$	2.807	0.689	2.954	0.507	0.743
$T_{0,Lim}$	0.299	0.124	0.295	0.030	0.243
$T_{d,Lim}$	0.353	0.118	0.336	0.042	0.360
$K_{g,Clay}$	0.026	0.019	0.035	0.009	0.469
$K_{g,add}$	0.433	0.263	0.474	0.140	0.533
$T_{0,Clay}$	0.352	0.127	0.366	0.022	0.172
$T_{d,Clay}$	0.326	0.161	0.321	0.037	0.231
	2008				
$K_{g,Lim}$	2.090	0.458	2.303	0.245	0.534
$T_{0,Lim}$	0.233	0.048	0.258	0.014	0.292
$T_{d,Lim}$	0.345	0.109	0.319	0.035	0.320
	2007				
$K_{g,Lim}$	1.873	0.481	2.067	0.238	0.492
$T_{0,Lim}$	0.238	0.093	0.282	0.018	0.197
$T_{d,Lim}$	0.369	0.107	0.330	0.028	0.265
	2006				
$K_{g,Lim}$	1.935	0.450	2.111	0.209	0.466
$T_{0,Lim}$	0.246	0.065	0.274	0.015	0.231
$T_{d,Lim}$	0.361	0.116	0.324	0.032	0.278

From this Table the following conclusions can be extracted:

- The selection of sample size M=14 outperforms of the one of M ≥ 14
- As concerns the gain parameters, the ratio of σ_{nat} (M=14) / σ_{nat} (M ≥ 14) is found in the range of 0.466 to 0.743.
- The range of the time constant and delay time respective ratios is from 0.172 to 0.360
- The gain values for M=14 are always higher from the ones for M ≥ 14. If the analysis of the section 3.2 is considered for the effect of the disturbances on the estimated gain, then it is derived that the gains estimated in the first case are more precise.

Consequently the selection of a small but adequate data set size provides average parameters of less uncertainty and the off line design of a robust controller becomes more effective. Also due to the smaller range between consecutive in time parameters, the MPC also design is expected to be of higher efficiency. A model predictive control can be applied as following:

(i) From the last M pairs of data, the model parameters are estimated.

(ii) If the model regression coefficient is $R \geq R_{min}$, then using these values and by implementing a standard or special technique, the optimum controller is determined. If $R < R_{min}$, the previous parameters or the average ones can be considered

(iii) The controller output is applied for the next time interval.

As the model parameters are up to now computed for time intervals of continuous raw mill operation, a question arises what parameters could be used, from the RM startup up to the moment that M reach a predefined value. To notice that usually the RM stop only for some hours. A solution can be to use average or the previously applied parameters. Another solution could be to use all the data sets – continuous and discontinuous in time - of size M, taking also data before and after the RM stoppage. In this case it shall be studied if the model has the same or similar reliability as the uninterrupted in time one studied up to now. This investigation is performed for the LSF transfer function. For comparison the next criteria are considered:

- The percentage of the sets population with R ≥ 0.7
- The average parameter value and the implied natural deviation σ_{nat}. To assure the validity of the results, several years data sets are processed. The results are shown in Table 3.

Table 3. Comparison of continuous time sets and total population of sets

	Average	σ_{nat}	Average	σ_{nat}
	Cont. time sets		All the sets	
	2009			
Number	1155		4871	
%Sets of R ≥ 0.7	45.7		46.4	
$K_{g,Lim}$	2.954	0.507	2.868	0.462
$T_{0,Lim}$	0.295	0.030	0.300	0.017
$T_{d,Lim}$	0.336	0.042	0.332	0.026
	2008			
Number	2024		5894	
%Sets of R ≥ 0.7	70.3		65.5	
$K_{g,Lim}$	2.303	0.245	2.238	0.232
$T_{0,Lim}$	0.258	0.014	0.268	0.014
$T_{d,Lim}$	0.319	0.035	0.313	0.030

Table 3 cont. Comparison of continuous time sets and total population of sets

	Average	σ_{nat}	Average	σ_{nat}
	Cont. time sets		All the sets	
	2007			
Number	2516		6088	
%Sets of $R \geq 0.7$	62.6		60.9	
$K_{g,Lim}$	2.067	0.238	2.043	0.232
$T_{0,Lim}$	0.282	0.018	0.290	0.014
$T_{d,Lim}$	0.330	0.028	0.329	0.029
	2006			
Number	3498		6607	
%Sets of $R \geq 0.7$	68.7		69.0	
$K_{g,Lim}$	2.111	0.209	2.096	0.210
$T_{0,Lim}$	0.274	0.015	0.287	0.012
$T_{d,Lim}$	0.324	0.032	0.327	0.023

The results of the Table 3 indicate that in spite the discontinuity of the data, the dynamics is not interrupted as the fraction of the total sets presenting $R \geq 0.7$ is comparable with that of continuous in time sets. This conclusion is very important in the case that MPC is selected as control strategy: From the last M data the dynamics is estimated and utilized to determine the control law to be applied to next time interval, if $R \geq R_{min}$. If $R < R_{min}$, then a previous or an average dynamics can be used.

3.5 Distribution of the Model Parameters

To have a more comprehensible representation of the model parameters uncertainty, the frequency and cumulative distributions of the gains are determined. The continuous time data sets of 2009 are selected with size M=14. The results are depicted in Figures 22, 23, 24.

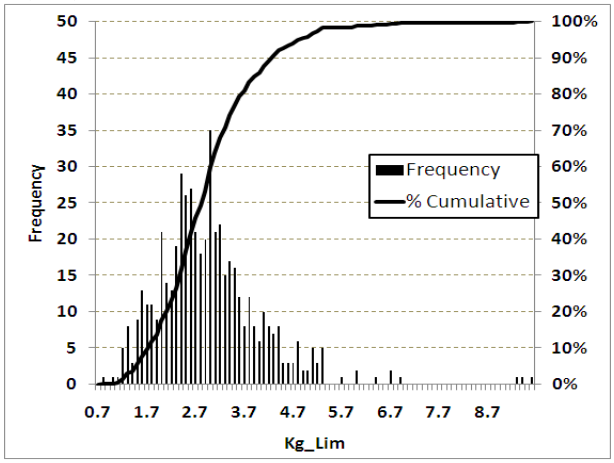

Figure 22. Gain from %Limestone to LSF

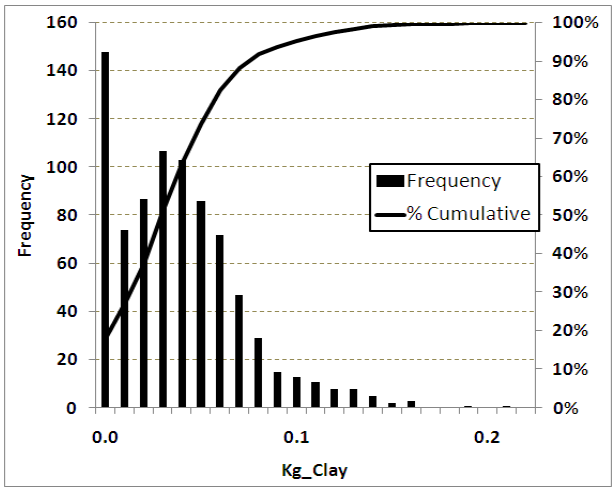

Figure 23. Gain from %Clay to SM

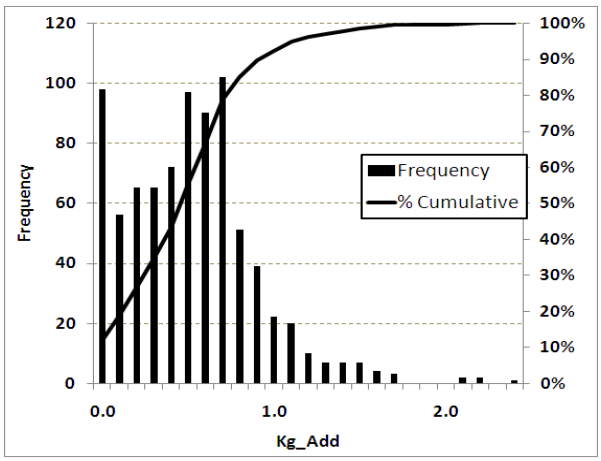

Figure 24. Gain from %Additive to SM

From these three figures the high level of uncertainty of the model parameters becomes clear. Additionally the gain of the transfer functions from %Clay and %Additive to SM does not follow a normal distribution as the $k_{g,Lim}$ does. It is verified that the enlarged disturbances cause a substantial uncertainty to the determination of the model parameters. Subsequently it becomes evident that advanced automatic control techniques are necessary to reject the mentioned disturbances.

After the implementation of the convolution theorem given by equation (12) to the models (9) and (10), the measured LSF_M or SM_M in time I+1, corresponding to the average sample between the times I and I+1, becomes a linear function of the feeders settings applied during the times I to I-N. These functions are given by the formulae (17) to (18):

$$LSF_{I+1} - LSF_0 = k_{g,Lim} \cdot \sum_{I=0}^{N} b_{I,Lim} \cdot (Lim_I - Lim_0) \quad (17)$$

$$SM_{I+1} - SM_0 = k_{g,Clay} \cdot \sum_{I=0}^{N} b_{I,Clay} \cdot (Clay_I - Clay_0) + k_{g,Add} \cdot \sum_{I=0}^{N} b_{I,Add} \cdot (Add_I - Add_0) \quad (18)$$

Where:

$$b_{I,x} = a_{I-1,x} \cdot \frac{t_M}{T_s} + a_{I,x} \cdot \left(1 - \frac{t_M}{T_s}\right) \; I = 0..N \quad (19)$$

Where x = Lim, Clay or Add. If I = 0, then the second term of the right member of the equation (19) is valid, while if I = N, only the first term is valid. The coefficients $\alpha_{I,x}$ are functions of time t_I and computed from the equations (20) - (22):

$$t_{I+1} = (I+1) \cdot T_s - t_M \quad I = 0..N \quad (20)$$

$$a_{0,x} = 1 - \left(1 + \frac{t_1 - t_{d,x}}{T_{0,x}}\right) \cdot exp\left(-\frac{t_1 - t_{d,x}}{T_{0,x}}\right) \quad (21)$$

$$a_{I,x} = \left(1 + \frac{t_I - t_{d,x}}{T_{0,x}}\right) \cdot exp\left(-\frac{t_I - t_{d,x}}{T_{0,x}}\right) - \left(1 + \frac{t_{I+1} - t_{d,x}}{T_{0,x}}\right) \cdot exp\left(-\frac{t_{I+1} - t_{d,x}}{T_{0,x}}\right) \; I = 1..N-1 \quad (22)$$

A common delay time and time constant is considered for x = clay or additive in the case of the linear model (18). The $Clay_0$ is determined from the balance: $Clay_0$=100-Lim_0-Add_0. The total of the coefficients $\alpha_{I,x}$ is equal to 1. The same is also valid for the coefficients $b_{I,x}$. For the computed range of the delay time and time constant, a population of past data N=4 is adequate to provide a sum of the coefficients equal to 1. Therefore by assuming constant composition of the raw material within each time interval T_s, the model of equations (7) to (12) results in the linear model of the formulae (17) to (22). Using these equations, the propagation of t_d and T_0 uncertainty to the coefficients α_I and b_I can be determined, by choosing the following approach:

(i) The average and σ_{Nat} of each time parameter is considered for the continuous in time sets of 2009 of a size M=14.

(ii) Using a random generator, random numbers are generated between 0 and 1.

(iii) Using the normal probability function and the random numbers as probabilities, sets of parameters are produced, using as normal distribution coefficients, the average and standard deviation considered in step (i)

(iv) The equations (19) to (22) are applied for each set of t_d, T_0 and the coefficients α_I and b_I are derived.

(v) The average value and the respective standard deviation of α_I and b_I are computed

(vi) The results are depicted in Table 4.

Table 4. α_I and b_I coefficients

Limestone coefficients					
	T_0			t_d	
Aver.(h)	0.295			0.336	
σ_{Nat}	0.030			0.043	
	α_0	α_1	α_2	α_3	
Aver.	0.260	0.669	0.066	0.004	
std. dev	0.054	0.036	0.023	0.003	
	b_0	b_1	b_2	b_3	b_4
Aver.	0.152	0.499	0.317	0.030	0.002
std. dev	0.032	0.009	0.025	0.011	0.001
Clay and Additive coefficients					
	T_0			t_d	
Aver.(h)	0.366			0.321	
σ_{Nat}	0.022			0.037	
	α_0	α_1	α_2	α_3	
Aver.	0.121	0.723	0.139	0.015	
std. dev	0.023	0.017	0.019	0.004	
	b_0	b_1	b_2	b_3	b_4
Aver.	0.071	0.472	0.382	0.067	0.006
std. dev	0.032	0.012	0.011	0.011	0.002

As it is observed form Table 4, the uncertainty of α_I and b_I and of T_0 and t_d are in the same range and not elevated.

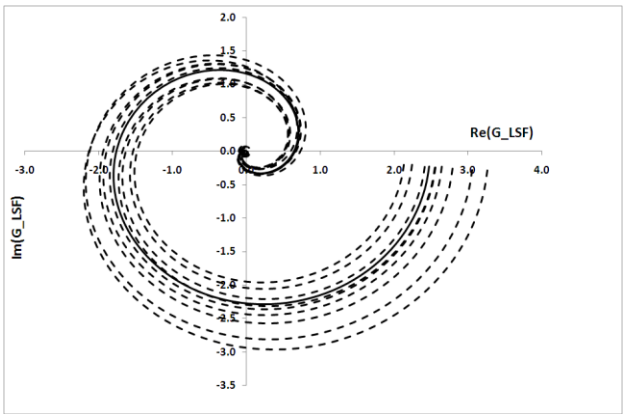

Figure 25. Nyquist plots of the %Limestone to LSF transfer function.

To investigate the impact of the parameters uncertainty on the Nyquist plot of the transfer

functions, the function from %Limestone to LSF is chosen and the steps (i) to (iii) of the previous procedure are initially applied. Then for each set of parameters $k_{g,Lim}$, T_0, t_d the Nyquist plot is derived. The results are shown in Figure 25. The solid line represents the average model parameters while with the dashed lines the transfer functions generated with the described procedure are depicted.

From this figure the large impact of the parameters uncertainty on the process transfer function is proved. The above results verify the necessity to include robustness criteria in the procedure of the controller design.

4 Conclusions

The dynamics of raw materials mixing in raw meal grinding systems is modeled effectively, by considering the transfer functions between the raw meal chemical moduli and the material proportions to the feeders. The sampling procedure and the delay time for sample preparation and analysis are taken into account. The process model is constituted from three transfer functions including five independent parameters each one. To compute these parameters with the maximum possible reliability a full year industrial data are collected and a specific algorithm is implemented. The results prove that the parameters uncertainty is elevated enough due to the large number of unpredicted disturbances during the raw meal production. Consequently advanced control theory and techniques are needed to attenuate the impact of these disturbances on the raw meal quality. The model developed can feed these tools with the results presented in order a robust controller to be achieved. The same technique to model the raw meal blending can also be applied to raw mills of the same or similar technology.

References:

[1] Lee, F.M., The Chemistry of Cement and Concrete,*3rd ed. Chemical Publishing Company, Inc.*, New York, 1971, pp. 164-165, 171-174, 384-387.

[2] Ozsoy, C. Kural, A. Baykara, C. , Modeling of the raw mixing process in cement industry, *Proceedings of 8th IEEE International Conference on Emerging Technologies and Factory Automation*, 2001, Vol. 1, pp. 475-482.

[3] Kural, A., Özsoy, C., Identification and control of the raw material blending process in cement industry, *International Journal of Adaptive Control and Signal Processing*, Vol. 18, 2004, pp. 427-442.

[4] Keviczky, L., Hetthéssy, J., Hilger, M. and Kolostori, J., Self-tuning adaptive control of cement raw material blending, *Automatica*, Vol. 14, 1978, pp.525-532.

[5] Banyasz, C. Keviczky, L. Vajk, I. A novel adaptive control system for raw material blending process, *Control Systems Magazine*, Vol. 23, 2003, pp. 87-96.

[6] Duan, X., Yang, C., Li, H., Gui, W., Deng, H., Hybrid expert system for raw materials blending, *Control Engineering Practice*, Vol. 16, 2008, pp. 1364-1371.

[7] Tsamatsoulis, D., Development and Application of a Cement Raw Meal Controller, *Ind. Eng. Chem. Res.*, Vol. 44, 2005, pp. 7164-7174.

[8] Gordon, L., Advanced raw mill control delivers improved economic performance in cement production, *IEEE Cement Industry Technical Conference*, 2004, pp. 263-272.

[9] Jing, J., Yingying, Y., Yanxian, F., Optimal Sliding-mode Control Scheme for the Position Tracking Servo System, *WSEAS Transactions on Systems*, Vol. 7, 2008, pp. 435-444.

[10] Bagdasaryan, A., System Approach to Synthesis, Modeling and Control of Complex Dynamical Systems, *WSEAS Transactions on Systems and Control*, Vol. 4, 2009, pp. 77-87.

[11] Emami, T., Watkins, J.M., A Unified Approach for Sensitivity Design of PID Controllers in the Frequency Domain, *WSEAS Transactions on Systems and Control*, Vol. 4, 2009, pp. 221-231.

[12] Emami, T., Watkins, J.M., Robust Performance Characterization of PID Controllers in the Frequency Domain, *WSEAS Transactions on Systems and Control*, Vol. 4, 2009, pp. 232-242.

[13] Tsamatsoulis, D., Dynamic Behavior of Closed Grinding Systems and Effective PID Parameterization, *WSEAS Transactions on Systems and Control*, Vol. 4, 2009, pp. 581-602.

[14] ISO 8258:1991, Shewhart Control Charts, *Statistical Methods for Quality Control*, Vol. 2, 1995, pp. 354-383.